ภาคผนวก

Research Article

SCI

Received: 10 October 2013 Revised: 6 January 2014 Accepted article published: 3 February 2014 Published online in Wiley Online Library:

(wileyonlinelibrary.com) DOI 10.1002/pi.4719

Trimethylsilyl-substituted triazole-based ligand for copper-mediated single-electron transfer living radical polymerization of methyl methacrylate

Preeyanuch Sangtrirutnugul,[a,b]* Kritdikul Wised,[a,b] Purmpoon Maisopa,[a,b] Nisalak Trongsiriwat,[a,b] Pramuan Tangboriboonrat[c] and Vichai Reutrakul[b]

Abstract

The tripodal 'click' compound tris(4-trimethylsilylmethyl-1,2,3-triazolylmethyl)amine (TTTA) was prepared and investigated as a ligand for copper-catalysed single-electron transfer living radical polymerization of methyl methacrylate (MMA). Bulk polymerizations catalysed by $Cu^0/CuBr_2$/TTTA with a molar ratio of $[MMA]_0/[ethyl\text{-}2\text{-}bromoisobutyrate]_0/[CuBr_2]_0/[TTTA]_0 = 200:2:1:1$ and a $1.0 \times 1.0\ cm^2$ Cu^0 sheet were fast and well controlled (76% conversion with $M_w/M_n = 1.19$ after 3.5 h). Greater amounts of added air generally gave slower polymerizations although M_w/M_n remained low (<1.3) even when the polymerization was carried out under aerobic conditions. Decreasing initial concentrations of the $Cu^0/CuBr_2$/TTTA catalyst system or polymerization temperatures also resulted in slower polymerizations and yielded polymers with broader dispersity. Kinetic studies in the temperature range 40–90 °C revealed an apparent activation energy of 22.6 kJ mol^{-1}.

Keywords: SET-LRP; copper catalyst; triazole ligand; activation energy; kinetics

INTRODUCTION

Metal-catalysed controlled/living radical polymerization (LRP)[1] first reported by Otsu in 1990 has become one of the most widely investigated polymerization techniques. Examples of metal-catalysed LRP include atom transfer radical polymerization (ATRP)[2,3] and single-electron transfer (SET) LRP.[4,5] Advantages of these processes include high functional group tolerance and an ability to afford polymers with controlled molecular weights, well-defined architectures and narrow molecular weight distributions.[6–11] Despite these favourable characteristics, a major limitation associated with normal copper-catalysed ATRP is the sensitivity to oxygen from the air, which can inhibit polymerization as a result of irreversible oxidation of Cu^I or formation of inactive peroxy radicals.[12] In addition, for certain systems, an overly active Cu^I catalyst rapidly converts to the persistent radical Cu^{II}–X and generates a high concentration of propagating radicals ($R^•$).[9] This event inevitably leads to radical termination and consequently large polymer masses with low monomer conversions.[13]

In comparison, SET-LRP, which features heterogeneous Cu^0 in the polymerization system, is more tolerable to oxygen and thus appears more attractive for large-scale polymer production. Proposed by Percec and co-workers, the SET-LRP mechanism involves activator Cu^0, in powder or wire form, which promotes heterolytic C–X bond cleavage of an initiator and a dormant polymer chain via an outer-sphere electron transfer to produce Cu^IX/L and the propagating radical ($R^•$) (Scheme 1). The key step in this mechanism is disproportionation of the *in situ* generated Cu^IX/L into the activator Cu^0/L and the deactivator $Cu^{II}X_2/L$. The $Cu^{II}X_2/L$ species reversibly deactivates $R^•$ to produce the dormant species R–X and regenerate Cu^IX/L. However, an alternative mechanism proposed by Matyjaszewski and co-workers is called activators regenerated by electron transfer ATRP.[14–20] In this mechanism, Cu^IX/L activates alkyl halides to give the propagating radicals ($R^•$) while Cu^0 serves as a heterogeneous reducing agent converting the persistent radical $Cu^{II}X_2/L$ to the activator Cu^IX/L. Furthermore, Cu^0 may also react directly with alkyl halides to give Cu^IX/L and $R^•$.[21–23] Generally for both mechanisms, Cu^0 acts as oxygen scavenger making the radical polymerization system less sensitive to air.[14,24–29]

We have been interested in investigating triazole-based compounds as catalyst supports in copper-catalysed ATRP. Despite the well-established chemistry of copper-catalysed azide–alkyne cycloadditon (CuAAC), applications of its 1,2,3-triazole products as ligands in catalysis are relatively limited.[30–36] Although previous studies have employed CuAAC in polymer synthesis,[37] only a few

* *Correspondence to: Preeyanuch Sangtrirutnugul, Center for Catalysis, Department of Chemistry, Faculty of Science, Mahidol University, Rama VI Road, Bangkok 10400, Thailand. E-mail: preeyanuch.san@mahidol.ac.th*

a *Center for Catalysis, Department of Chemistry, Faculty of Science, Mahidol University, Rama VI Road, Bangkok 10400, Thailand*

b *Department of Chemistry and Center of Excellence for Innovation in Chemistry, Faculty of Science, Mahidol University, Rama VI Road, Bangkok 10400, Thailand*

c *Department of Chemistry, Faculty of Science, Mahidol University, Rama VI Road, Bangkok 10400, Thailand*

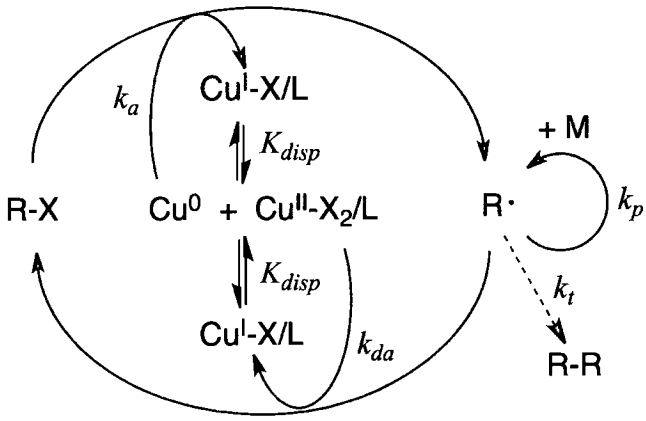

Scheme 1. Proposed mechanism for SET-LRP.

examples of copper catalysts supported by 1,2,3-triazole ligands in radical polymer synthesis are known.[38,39] In SET-LRP, ligands are expected to influence the disproportionation equilibrium of Cu^{I}X/L and stabilize the colloidal Cu^0 activator.[5] Despite these crucial roles, not many N-ligand types have so far been investigated.[40] Since the substituents at the triazole ring can be conveniently varied depending on the organic azides and terminal alkynes used, solubility and redox properties of the copper complexes can be systematically tuned and, as a result, polymer properties can be manipulated. Our group has recently reported the use of the tripodal triazole-based ligands tris(4-R-1,2,3-triazolylmethyl)amine (R = CH_2Ph (TBTA), CH_2Fc (TFcTA)) for copper-catalysed normal ATRP.[39] However, a major drawback of the Cu^{I}Br/TBTA and Cu^{I}Br/TFcTA catalysts is their low solubility in organic solvents, resulting in broad M_w/M_n values of the resulting polymers. To improve catalyst solubility in organic media and to increase the electron-donating ability, the more hydrophobic tripodal tris(4-trimethylsilylmethyl-1,2,3-triazolylmethyl)amine (TTTA) was prepared and evaluated as a support for Cu(II) deactivator in SET-LRP of methyl methacrylate (MMA).

EXPERIMENTAL

Materials

MMA (Merck, 99%) was dried with CaH_2 at room temperature for 2 days, distilled under vacuum and stored in a Teflon valve-sealed storage flask at −5 °C. Copper metal was scrubbed with sandpaper, washed with hexane and dried in an oven prior to use. Anisole was refluxed with Na under Ar and distilled under reduced pressure. Dimethylsulfoxide (DMSO; Lab Scan) was dried with CaH_2 and distilled under Ar. Trimethylsilylmethyl azide ($Me_3SiCH_2N_3$) was prepared according to a previous literature report.[41] $CuBr_2$ (Aldrich), tripropargylamine (Aldrich), trimethylsilylmethyl chloride (Me_3SiCH_2Cl; Merck), NaN_3 (Carlo Erba), ethyl-2-bromoisobutyrate (EBiB; Aldrich) and L-(+)-ascorbic acid (Riedel-de Haën) were purchased and used as received.

^{1}H NMR (500 MHz), ^{13}C{^{1}H} NMR (125 MHz) and ^{29}Si{^{1}H} NMR (99 MHz) spectra were acquired using a Bruker AV-500 spectrometer equipped with a 5 mm proton/BBI probe. All NMR spectra were recorded at room temperature and referenced to protic impurities in the deuterated solvent for ^{1}H, solvent peaks for ^{13}C{^{1}H} and $Si(CH_3)_4$ for ^{29}Si{^{1}H}. Elemental analyses were conducted at the Chemistry Department, Mahidol University.

Synthesis and characterization

TTTA. Tripropargylamine (0.91 mL, 6.4 mmol) was treated with 3.3 eq. of $Me_3SiCH_2N_3$ (2.8 g, 22 mmol) in a 1:1 mixture of CH_2Cl_2–H_2O (50 mL) with 15 mol% of $CuSO_4{\cdot}5H_2O$ (1.0 mol L^{-1}, 1.0 mL, 1.0 mmol) and 45 mol% of ascorbic acid (0.51 g, 2.9 mmol). After 24 h, 30 mL of distilled water was added to the reaction mixture, after which the aqueous layer was extracted with 3 × 30 mL of CH_2Cl_2. To the combined organic layer was added ethylenediaminetetraacetic acid (0.32 g, 1.1 mmol) in 10% aqueous solution of NH_3 (170 mL). The resulting mixture was stirred for 3 h and the CH_2Cl_2 solution was washed with 3 × 30 mL of distilled water. Then, the CH_2Cl_2 solution was dried over anhydrous Na_2SO_4. Recrystallization in diethyl ether afforded the product TTTA in 74% yield (2.4 g, 4.7 mmol). ^{1}H NMR (500 MHz, $CDCl_3$; δ, ppm): 7.65 (s, 3H; C*H*=N), 3.91 (s, 6H; NCH_2), 3.71 (s, 6H; CH_2Si), 0.13 (s, 27H; SiCH_3). ^{13}C{^{1}H} NMR (125 MHz, $CDCl_3$; δ, ppm): 143.5, 124.4 (triazole carbons), 46.9 (CH_2), 41.8 (CH_2), 2.6 (CH_3). ^{29}Si{^{1}H} NMR (99 MHz, $CDCl_3$; δ, ppm): 2.3 (s). Analysis: calcd for $C_{21}H_{42}N_{10}Si_3$: C 48.61, H 8.16, N 26.99; found: C 48.27, H 8.10, N 27.12.

$CuBr_2$/TTTA. Reaction of TTTA (0.20 g, 0.38 mmol) with $CuBr_2$ (0.094 g, 0.42 mmol) was carried out in CH_2Cl_2 under Ar at room temperature. After 5 h, the dark green solution was dried *in vacuo*. Recrystallization in ethyl acetate resulted in a green microcrystalline solid in 57% yield (0.18 g, 0.24 mmol). ^{1}H NMR (500 MHz, $CDCl_3$; δ, ppm): 4.20 (br s, 6H; CH_2Si), 0.22 (br s, 27H; SiCH_3). ^{29}Si{^{1}H} NMR (99 MHz, $CDCl_3$; δ, ppm): −7.0 (s). Analysis: calcd for $C_{21}H_{42}N_{10}Br_2CuSi_3$: C 33.98, H 5.70, N 18.87; found: C 33.90, H 5.63, N 18.77.

Cyclic voltammetry (CV)

CV was carried out at ambient temperature with an Autolab PGSTAT 30 potentiostat and GPES software. The Cu^{II} complex $CuBr_2$/TTTA (1.0 mmol L^{-1}) was dissolved in dry DMSO containing 0.1 mol L^{-1} [Et_4N][PF_6] electrolyte. Measurements were performed under Ar at a scanning rate of 0.01 V s^{-1} with a glassy carbon working electrode, a platinum counter electrode and an Ag/Ag$^+$ reference electrode. The sample was referenced to the ferrocene internal standard and its potential was reported *versus* those of Fc/Fc$^+$.

General procedure for SET-LRP of MMA

To a dried Schlenk tube equipped with a magnetic stir bar were added TTTA (48 mg, 0.093 mmol) and $CuBr_2$ (21 mg, 0.093 mmol) under Ar. Then, 2.0 mL of MMA (19 mmol) was added. The reaction flask was tightly closed and the solution mixture was degassed with three freeze–pump–thaw cycles using dry ice–acetone. Under an Ar flow, a copper sheet (size of 0.5 × 0.5, 1.0 × 1.0 or 1.5 × 1.5 cm^2) was added to the frozen reaction mixture after which the system was evacuated and refilled with Ar five times. Next, the reaction mixture was allowed to thaw, to which anisole (200 μL), used as an internal standard, was added. After 10 min at room temperature, EBiB (30 μL, 0.19 mmol) was added via a syringe to initiate the polymerization. The reaction flask was immediately immersed in a pre-heated oil bath. After a given time, approximately 20 mL of tetrahydrofuran (THF) was added to stop the polymerization, after which the Schlenk tube was cooled at −78 °C for 5 min. The resulting polymer was precipitated using *ca* 200 mL of CH_3OH.

SET-LRP of MMA in the presence of air

Polymerizations with added air followed the general procedure for SET-LRP. A certain volume of air was introduced to the reaction

flask via a syringe immediately after immersing the reaction tube in the pre-heated oil bath. The septum was then wrapped with electrical tape and Parafilm®. In the case of polymerizations under aerobic conditions, the reaction mixture was not degassed using the freeze–pump–thaw technique and the polymerization was carried out in air.

Polymerization characterization

Based on ^{1}H NMR spectroscopy, monomer conversions were determined by comparing the $-OCH_3$ peak area of poly(methyl methacrylate) (PMMA) to the $-OCH_3$ integration of the anisole reference. Molecular weight distributions of polymer were measured using a Waters e2695 system equipped with PLgel 10 mm mixed B 2 columns (molecular weight resolving range = 500–10 000 g mol^{-1}). As eluent, THF was used at a flow rate of 1 mL min^{-1} at 40 °C with calibration based on PMMA standards.

Kinetic experiments

Kinetic studies were performed in neat MMA under similar conditions as described for SET-LRP, except that the amounts used were three times that of typical SET-LRP (0.28 mmol of $CuBr_2$ and TTTA, three appropriately sized copper sheets, 600 μL of anisole, 6.0 mL of MMA and 90 μL of EBiB). After a given time, approximately 0.5 mL of a sample was withdrawn using a syringe to determine monomer conversions, polymer molecular weights and polydispersity index (PDI) via ^{1}H NMR spectroscopy and gel permeation chromatography (GPC) analysis, respectively.

RESULTS AND DISCUSSION

Synthesis of tripodal click ligand (TTTA) and $CuBr_2$/TTTA complex

Reaction of $N(CH_2CCH)_3$ and 3 eq. of $Me_3SiCH_2N_3$ in a 1:1 mixture of CH_2Cl_2–H_2O at room temperature afforded TTTA as a white solid which was crystallized from diethyl ether in 74% yield (Scheme 2). The ^{1}H NMR spectrum of TTTA ($CDCl_3$) contains a characteristic *CH* (triazole) singlet resonance at 7.9 ppm whereas the $SiMe_3$ group signal appears at 0.16 and 2.3 ppm in the ^{1}H NMR and ^{29}Si{^{1}H} NMR spectra, respectively.

Treatment of TTTA with 1 eq. of $CuBr_2$ in CH_2Cl_2 at room temperature readily produced the corresponding dark green Cu^{II} complex, $CuBr_2$/TTTA. Crystallization of $CuBr_2$/TTTA in ethyl acetate afforded a green microcrystalline solid in 57% yield. Due to the paramagnetic nature of the Cu^{II} complex, its ^{1}H NMR spectrum in $CDCl_3$ reveals broad resonances at 4.2 and 0.22 ppm, corresponding to CH_2Si and $Si(CH_3)_3$, respectively. The ^{29}Si{^{1}H} NMR spectrum contains a singlet resonance at −7.0 ppm. It should be noted that the crystal structure of the related complex $[Cu^{II}Cl(TBTA)][Cl]$ has previously been reported showing a distorted trigonal bipyramidal structure with an outer-sphere chloride ion.[42]

Table 1. CV data of $CuBr_2$/L in DMSO[a]

Entry	Complex	$E_{p,a}$ (V)	$E_{p,c}$ (V)	ΔE_p (mV)	$E_{1/2}$[b] (V)
1	$CuBr_2$/TTTA	−0.206	−0.338	132	−0.272
2[c]	$CuBr_2$/TBTA	−0.0885	−0.324	235	−0.206
3[c]	$CuBr_2$/TFcTA[d]	−0.0625	−0.386	324	−0.224

[a] 0.1 mol L^{-1} $[NBu_4][PF_6]$, 1.0 mmol L^{-1} $CuBr_2$/L; scan rate, 0.01 V s^{-1}; potentials reported *versus* Fc/Fc^+; $E_{p,a}$ and $E_{p,c}$ are the peak potentials of the oxidation and reduction waves, respectively.
[b] $E_{1/2} = (E_{p,a} + E_{p,c})/2$.
[c] Sangtrirutnugul *et al.*[39]
[d] Fe(II)/Fe(III) redox potentials of the ferrocenyl substituents are not shown.

CV of $CuBr_2$/TTTA was carried out in DMSO and referenced to the ferrocene internal standard. The CV profile of $CuBr_2$/TTTA reveals a quasi-reversible Cu^I/Cu^{II} redox wave at $E_{1/2} = -0.272$ V with a cathodic–anodic peak separation (ΔE_p) of 132 mV (Table 1, entry 1). In comparison to the previously reported values of tripodal click analogues TBTA and TFcTA (Table 1, entries 2 and 3), the trimethylsilyl-substituted tripodal ligand (TTTA) exhibited stronger electron-donating ability based on a lower $E_{1/2}$ value.

SET-LRP of MMA with $Cu^0/CuBr_2$/TTTA

Bulk polymerizations of MMA were catalysed by a 1.0 × 1.0 cm^2 Cu^0 sheet ($[Cu^0] = 0.90$ cm^2 mL^{-1}) in the presence of $CuBr_2$/TTTA using a molar ratio of $[MMA]_0/[EBiB]_0/[CuBr_2]_0/[TTTA]_0 = 200:2:1:1$. Heating the reaction mixture at 90 °C initially results in a homogeneous green solution, indicative of Cu^{II} species. After a while, the polymerization mixture turns slightly cloudy and pale yellow in colour, which can be attributed to the *in situ* reduction of Cu^{II} to Cu^I species. It is found that, in the presence of TTTA ligand, an effective SET-LRP of MMA in bulk is achieved as 76% yield of PMMA (PDI = 1.19) is obtained (Table 2, entry 3).

In addition, when the Cu^IBr/TTTA catalyst is used, a negligible amount of polymer product is isolated after 24 h. On the other hand, without $Cu^{II}Br_2$, the Cu^0/TTTA catalyst system results in poorly controlled polymerization with high polymer mass and M_w/M_n value (Table 2, entry 1). Based on these results, Cu^0 is proposed as the active catalyst, which directly activates the C–Br bond, whereas the deactivator $Cu^{II}Br_2$ is crucial to achieve well-controlled polymerizations.

The effect of Cu^0 areas was investigated, as shown in entries 2–4 of Table 2. While the polymerization systems using 1.5 × 1.5 cm^2 ($[Cu^0] = 2.0$ cm^2 mL^{-1}) and 1.0 × 1.0 cm^2 ($[Cu^0] = 0.90$ cm^2 mL^{-1}) Cu^0 sheets result in similar polymer yields, the smaller Cu^0 area of 0.5 × 0.5 cm^2 ($[Cu^0] = 0.22$ cm^2 mL^{-1}) results in slower polymerization. This observation is supported by kinetic studies, which reveal first-order kinetic plots and comparable observed polymerization rate constants ($k_{obs} \sim 1.2 \times 10^{-4}$ s^{-1}) for all three Cu^0 surface areas

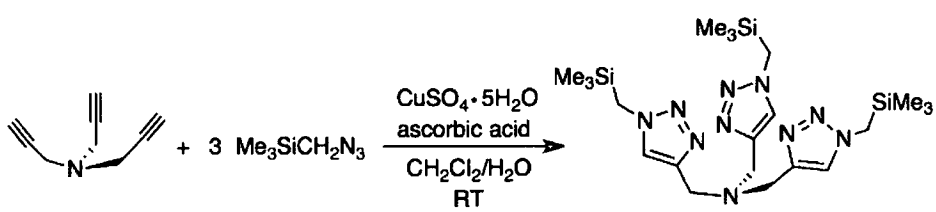

Scheme 2. Synthesis of tris(4-trimethylsilylmethyl-1,2,3-triazolylmethyl)amine (TTTA).

Table 2. SET-LRP of MMA using various amounts of Cu^0, $Cu^{II}Br_2$, EBiB and TTTA[a]

Entry	MMA	EBiB	Cu^0 sheet (cm^2)	Time (h)	Conv. (%)	$M_{n,th}$[b] ($g\,mol^{-1}$)	$M_{n,GPC}$ ($g\,mol^{-1}$)	PDI
1[c]	200	2	1.0 × 1.0	5.0	75	7 704	47 700	1.55
2	200	2	0.5 × 0.5[d]	5.0	82	8 405	18 400	1.16
3	200	2	1.0 × 1.0[e]	3.5	76	7 758	24 200	1.19
4	200	2	1.5 × 1.5[f]	2.8	68	7 038	29 500	1.13
5	400	2	1.0 × 1.0	3.5	76	15 413	26 200	1.25
6	400	4	1.0 × 1.0	6.0	85	5 802	11 700	1.37
7	1000	2	1.0 × 1.0	8.0	53	26 652	40 200	1.30
8	1000	10	1.0 × 1.0	11	45	4 700	8 200	1.35
9	2000	2	1.0 × 1.0	15	45	45 249	48 100	1.37
10[g]	2000	2	1.0 × 1.0	19	64	64 272	123 300	1.39

[a] Polymerization conditions: 90 °C; initiator, EBiB; molar ratio $[MMA]_0/[EBiB]_0/[CuBr_2]_0/[TTTA]_0$ = MMA:EBiB:1:1.
[b] $M_{n,th} = [([MMA]_0/[EBiB]_0) \times \%\ \text{conversion} \times M_{w,MMA}] + M_{w,EBiB}$.
[c] No $CuBr_2$ added.
[d] $[Cu^0] = 2.0\ cm^2\ mL^{-1}$.
[e] $[Cu^0] = 0.90\ cm^2\ mL^{-1}$.
[f] $[Cu^0] = 0.22\ cm^2\ mL^{-1}$.
[g] $[MMA]_0/[EBiB]_0/[CuBr_2]_0/[TTTA]_0 = 2000:2:1:3$.

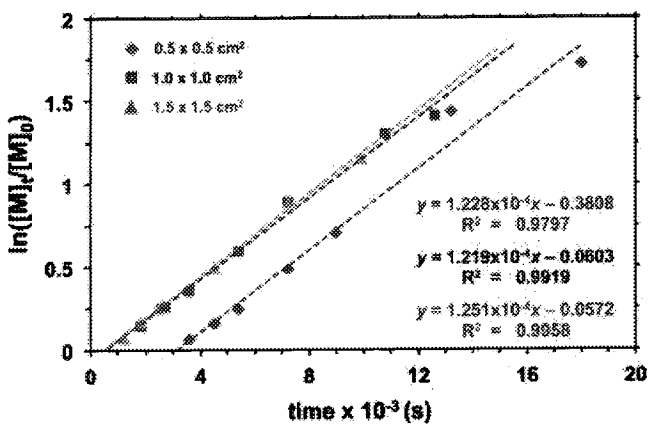

Figure 1. Kinetic plots of bulk polymerizations of MMA as a function of Cu^0 area (0.5 × 0.5 cm^2, 1.0 × 1.0 cm^2, 1.5 × 1.5 cm^2).

(Fig. 1). Although several previous studies have shown that increasing the amount of Cu^0 generally gives higher k_{obs} values,[14,43,44] Percec and co-workers have recently reported similar finding in which k_{obs} values are not significantly affected by changes in Cu^0 surface area.[45] It is possible that, under the polymerization conditions studied, the solution is already saturated with the active Cu^0 catalyst. The kinetic plots shown in Fig. 1 also reveal that the smallest Cu^0 area of 0.50 × 0.50 cm^2 ($[Cu^0] = 0.22\ cm^2\ mL^{-1}$) affords a longer induction period (52 min). In contrast, polymerization systems with 1.0 × 1.0 cm^2 and 1.5 × 1.5 cm^2 copper sheets ($[Cu^0] = 0.90$ and 2.0 $cm^2\ mL^{-1}$, respectively) surprisingly result in similar induction periods (*ca* 8 min). The reason for the discrepancy involving comparable induction periods for different Cu^0 surface areas (Table 2, entries 3 and 4) is still unclear and will be the subject of further study.

Effect of copper concentration

Due to the heterogeneity of SET-LRP, it should be possible to use a low starting amount of the $Cu^0/CuBr_2$/TTTA catalyst system.[46–48]

Table 3. Effect of added air on SET-LRP of MMA using $Cu^0/Cu^{II}Br_2$/TTTA[a]

Entry	Air (mL)	Time (h)	Conv. (%)	$M_{n,th}$[b] ($g\,mol^{-1}$)	$M_{n,GPC}$ ($g\,mol^{-1}$)	PDI
1	1.0	3.0	64	6 556	17 300	1.14
2	3.0	3.0	44	4 609	14 600	1.12
3	5.0	3.0	19	2 105	5 900	1.25
4	In air	9.0	53	5 573	22 900	1.21

[a] Polymerization conditions: 90 °C; initiator, EBiB; $[Cu^0] = 0.90\ cm^2\ mL^{-1}$; molar ratio $[MMA]_0/[EBiB]_0/[CuBr_2]_0/[TTTA]_0 = 200:2:1:1$ in bulk MMA.
[b] $M_{n,th} = [([MMA]_0/[EBiB]_0) \times \%\ \text{conversion} \times M_{w,MMA}] + M_{w,EBiB}$.

To investigate the effect of the amount of copper catalyst, higher monomer ratios of $[MMA]_0/[CuBr_2]_0/[TTTA]_0$ (400:1:1, 1000:1:1 and 2000:1:1) were used in the presence of a 1.0 × 1.0 cm^2 copper sheet. The polymerization data reveal that a decrease in $CuBr_2$/TTTA concentration (500 to 50 ppm) and $[Cu^0]$ (0.47 to 0.099 $cm^2\ mL^{-1}$) result in slower and less controlled polymerizations (PDI = 1.25–1.39) (Table 2, entries 5–10). An increase in the $[EBiB]_0/[MMA]_0$ ratio leads to no change in the polymerizations although lower polymer molecular weights are obtained (Table 2, entries 6 and 8). Along the same lines, the use of a threefold excess of TTTA does not have an apparent effect on the polymerization nor the PDI (Table 2, entry 10).

Effect of added air

Catalyst tolerance to oxygen is important for the industrialization of ATRP. Thus, controlled radical polymerizations in the presence of air were evaluated for this catalyst system. In general, oxygen from the air is known to oxidize Cu^I to the deactivator species $Cu^{II}Br_2/L$ and consequently to slow down the polymerization rates. Table 3 shows that greater amounts of injected air (i.e. 1.0, 3.0 and 5.0 mL; entries 1–3) indeed lead to reduced monomer conversions at 3 h although the polymerizations remain well controlled based on low PDI values in the range 1.12–1.25. In fact, for entry 4, MMA is polymerized under aerobic conditions using non-degassed MMA. In the presence of oxygen and moisture, the polymerization is slow and the reaction mixture appears viscous after 9 h. Despite relatively low monomer conversion (53%), a small PDI value of 1.21 is obtained, based on ^1H NMR spectra and GPC analysis.

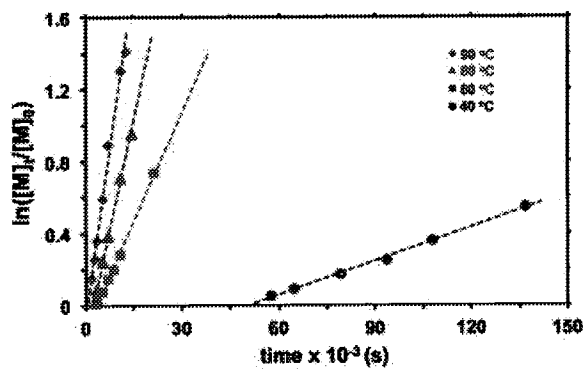

Figure 2. Kinetic plots of bulk polymerizations of MMA as a function of reaction temperature.

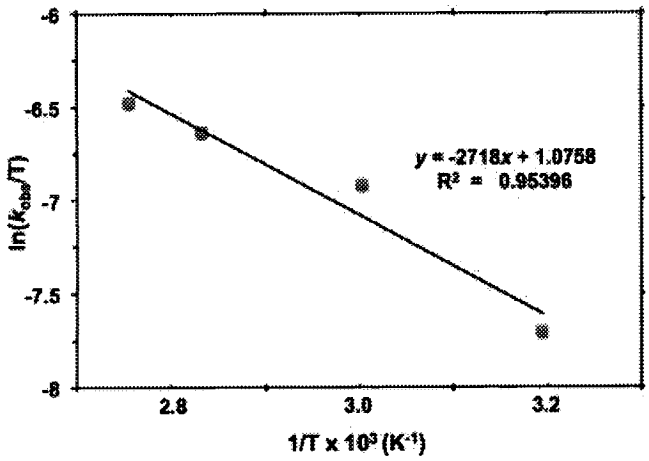

Figure 3. Arrhenius plot in the temperature range 40–90 °C.

Table 4. Effect of reaction temperature on SET-LRP of MMA using $Cu^0/Cu^{II}Br_2/TTTA$[a]

Entry	Temp. (°C)	Time (h)	Conv. (%)	$M_{n,th}$[b] (g mol^{-1})	$M_{n,GPC}$ (g mol^{-1})	f[c]	PDI	k_{obs} (s^{-1})
1	90	3.5	76	7758	24 200	0.32	1.19	1.22×10^{-4}
2	80	4.0	62	6387	20 600	0.31	1.23	8.12×10^{-5}
3	60	6.0	52	5427	35 900	0.15	1.30	4.02×10^{-5}
4	40	38	42	4393	57 000	0.08	1.40	6.24×10^{-6}

[a] Polymerization conditions: 90 °C; initiator, EBiB; $[Cu^0] = 0.90\,cm^2\,mL^{-1}$; molar ratio $[MMA]_0/[EBiB]_0/[CuBr_2]_0/[TTTA]_0 = 200:2:1:1$ in bulk MMA.
[b] $M_{n,th} = [([MMA]_0/[EBiB]_0) \times \%\ conversion \times M_{w,MMA}] + M_{w,EBiB}$.
[c] f (initiation efficiency) $= M_{n,th}/M_{n,GPC}$.

Effect of temperature and activation energy

The effect of temperature on catalyst activity and polymer properties was studied by varying the polymerization temperature (i.e. 40–90 °C). Figure 2 shows that, in all cases, first-order kinetic plots are obtained. In addition, observed rate constants of polymerization (k_{obs}) decrease at lower temperatures (Table 4). For the temperatures investigated, an induction period is present, which becomes longer as the polymerization temperature decreases. For example, at 90 °C, the induction period is 8 min compared to 14 h at 40 °C.

Based on these data, an Arrhenius plot of $\ln(k_{obs}/T)$ *versus* $1/T$ in the temperature range 40–90 °C was constructed as illustrated in Fig. 3, giving a calculated activation energy (E_a) of 22.6 kJ mol^{-1}. To the best of our knowledge, this is the first report of an apparent energy of activation of a copper-mediated SET-LRP system. However, there are previous reports of E_a values of normal copper-catalysed ATRP of MMA. For example, Mittal and Sivaram found the apparent activation energy of the Cu^IBr/2,6-bis[1-(2,6-diisopropylphenylimino)ethyl]pyridine catalyst for normal ATRP of MMA in toluene to be 51.0 kJ mol^{-1}.[49] Several other examples of E_a values for normal ATRP of MMA appear to be similar in the range 53–63 kJ mol^{-1}.[50–53] A low E_a value of 21.7 kJ mol^{-1} was obtained for normal ATRP of MMA catalysed by CuBr with the bidentate cyclopentyl-substituted pyridine-2-carboximidate ligand in 50 wt% veratrole solution.[54] On the basis of these values, the apparent activation energy of bulk polymerizations of MMA using the $Cu^0/CuBr_2$/TTTA catalyst system is considered very low, consistent with observed high catalyst activity compared to other ATRP systems.

CONCLUSIONS

We have demonstrated that TTTA is an effective ligand for copper-catalysed SET-LRP of MMA. In this work, the k_{obs} values were found to be independent of the Cu^0 surface area, possibly due to saturation of Cu^0 active species under the experimental conditions investigated. Bulk polymerizations of MMA in the presence of air were slow but well controlled, as evidenced by low polymer PDI values. Kinetic data for the polymerization temperature range 40–90 °C revealed longer induction periods with decreasing temperatures and relatively low apparent activation energy ($E_a = 22.6$ kJ mol^{-1}). These promising polymerization results coupled with ease of ligand synthesis and modification make the tripodal triazole-based derivatives of the type tris(4-R-1,2,3-triazolylmethyl)amine an attractive ligand class for copper-catalysed SET-LRP. Further modification of substituents at the triazole ring and optimization of polymerization conditions in order to improve monomer conversion and initiation efficiency of the system are ongoing.

ACKNOWLEDGEMENTS

The authors acknowledge the Thailand Research Fund and Commission on Higher Education for financial support under grant no. MRG5580036. This work was also supported by the Center of Excellence for Innovation in Chemistry (PERCH-CIC) and Faculty of Science, Mahidol University, and Mahidol University under the National Research Universities Initiative. We are grateful to Dr Waret Veerasai for his help with cyclic voltammetry.

REFERENCES

1 Otsu T, Yoshida M and Tazaki T, *Makromol Chem Rapid Commun* **3**:133–140 (1982).
2 Wang J-S and Matyjaszewski K, *J Am Chem Soc* **117**:5614–5615 (1995).
3 Kato M, Kamigaito M, Sawamoto M and Higashimura T, *Macromolecules* **28**:1721–1723 (1995).
4 Percec V, Guliashvili T, Ladislaw JS, Wistrand A, Stjerndahl A, Sienkowska MJ, *et al*, *J Am Chem Soc* **128**:14156–14165 (2006).
5 Rosen BM and Percec V, *Chem Rev* **109**:5069–5119 (2009).
6 Coessens V, Pintauer T and Matyjaszewski K, *Prog Polym Sci* **26**:337–377 (2001).
7 Kamigaito M, Ando T and Sawamoto M, *Chem Rev* **101**:3689–3745 (2001).
8 Matyjaszewski K, *Macromolecules* **45**:4015–4039 (2012).
9 Matyjaszewski K and Xia J, *Chem Rev* **101**:2921–2990 (2001).
10 Sarbu T, Lin K-Y, Ell J, Siegwart DJ, Spanswick J and Matyjaszewski K, *Macromolecules* **37**:3120–3127 (2004).
11 Tsarevsky NV and Matyjaszewski K, *Chem Rev* **107**:2270–2299 (2007).
12 Min K, Jakubowski W and Matyjaszewski K, *Macromol Chem Rapid Commun* **27**:594–598 (2006).
13 Fischer H, *Chem Rev* **101**:3581–3610 (2001).
14 Magenau AJD, Kwak Y and Matyjaszewski K, *Macromolecules* **43**:9682–9689 (2010).
15 Matyjaszewski K, Coca S, Gaynor SG, Wei M and Woodworth BE, *Macromolecules* **30**:7348–7350 (1997).
16 Matyjaszewski K, Dong H, Jakubowski W, Pietrasik J and Kusumo A, *Langmuir* **23**:4528–4531 (2007).
17 Matyjaszewski K, Pyun J and Gaynor SG, *Macromol Rapid Commun* **19**:665–670 (1998).
18 Matyjaszewski K, Woodworth BE, Zhang X, Gaynor SG and Metzner Z, *Macromolecules* **31**:5955–5957 (1998).
19 Queffelec J, Gaynor SG and Matyjaszewski K, *Macromolecules* **33**:8629–8639 (2000).
20 Sarbu T and Matyjaszewski K, *Macromol Chem Phys* **202**:3379–3391 (2001).

21 Matyjaszewski K, Tsarevsky NV, Braunecker WA, Dong H, Huang J, Jakubowski W, *et al*, *Macromolecules* **40**:7795–7806 (2007).
22 Van der Sluis M, Barboiu B, Pesa N and Percec V, *Macromolecules* **31**:9409–9412 (1998).
23 Hornby BD, West AG, Tom JC, Waterson C, Harrison S and Perrier S, *Macromol Rapid Commun* **31**:1276–1280 (2010).
24 Acar AE, Yagci MB and Mathias LJ, *Macromolecules* **33**:7700–7706 (2000).
25 Hizal G, Tunca U, Aras S and Mert H, *J Polym Sci A: Polym Chem* **44**:77–87 (2006).
26 Jakubowski W, Min K and Matyjaszewski K, *Macromolecules* **39**:39–45 (2006).
27 Kwak Y, Magenau AJD and Matyjaszewski K, *Macromolecules* **44**:811–819 (2011).
28 Matyjaszewski K, Dong H, Jakubowski W, Pietrasik J and Kusumo A, *Langmuir* **23**:4528–4531 (2007).
29 Nguyen NH and Percec V, *J Polym Sci A: Polym Chem* **49**:4756–4765 (2011).
30 Chan TR, Hilgraf R, Sharpless KB and Fokin VV, *Org Lett* **6**:2853–2855 (2004).
31 Detz RJ, Heras SA, de Gelder R, van Leeuwen PWNM, Hiemstra H, Reek JNH, *et al*, *Org Lett* **8**:3227–3230 (2006).
32 Duan H, Sengupta S, Petersen JL, Akhmedov NG and Shi X, *J Am Chem Soc* **131**:12100–12102 (2009).
33 Liu D, Gao W, Dai Q and Zhang X, *Org Lett* **7**:4907–4910 (2005).
34 Liang L and Astruc D, *Coord Chem Rev* **255**:2933–2945 (2011).
35 Li L, Gomes CSB, Gomes PT, Duarte MT and Fan Z, *Dalton Trans* **40**:3365–3380 (2011).
36 Jindabot S, Teerachana K, Thongkam P, Kiatisevi S, Khamnaen T, Phiriyawirut P, *et al*, *J Organomet Chem* **750**:35–40 (2014).
37 Meldal M, *Macromol Chem Rapid Commun* **29**:1016–1051 (2008).
38 Bergbreiter DE, Hamilton PN and Koshti NM, *J Am Chem Soc* **129**:10666–10667 (2007).
39 Sangtrirutnugul P, Maisopa P, Chaicharoenwimolkul L, Sunsin A, Somsook E and Reutrakul V, *J Appl Polym Sci* **127**:2757–2763 (2013).
40 Nguyen NH, Levere ME and Percec V, *J Polym Sci A: Polym Chem* **50**:35–46 (2012).
41 Tsuge O, Kanemasa S and Matsuda K, *Chem Lett* 1131–1134 (1983).
42 Donnelly PS, Zanatta SD, Zammit SC, White JM and Williams SJ, *Chem Commum* 2459–2461 (2008).
43 Nguyen NH, Rosen BM, Lligadas G and Percec V, *Macromolecules* **42**:2379–2386 (2009).
44 Lligadas G, Rosen BM, Bell CA, Monteiro MJ and Percec V, *Macromolecules* **41**:8365–8371 (2008).
45 Nguyen NH, Kulis J, Sun H-J, Jia Z, van Beusekom B, Levere ME, *et al*, *Polym Chem* **4**:144–155 (2013).
46 Nicolaÿ R, Kwak Y and Matyjaszewski K, *Angew Chem Int Ed* **49**:541–544 (2010).
47 Min K, Gao HF and Matyjaszewski K, *J Am Chem Soc* **127**:3825–3830 (2005).
48 Jakubowski W and Matyjaszewski K, *Angew Chem Int Ed* **45**:4482–4486 (2006).
49 Mittal A and Sivaram S, *J Polym Sci A: Polym Chem* **43**:4996–5008 (2005).
50 Wang J-L, Grimaud T and Matyjaszewski K, *Macromolecules* **30**:6507–6512 (1997).
51 Zhang H and Van Der Linde R, *J Polym Sci A: Polym Chem* **40**:3549–3561 (2002).
52 Noda T, Grice AJ, Levere ME and Haddleton DM, *Eur Polym J* **43**:2312–2330 (2007).
53 Haddleton DM, Kukulj D, Duncalf DJ, Heming AM and Shooter AJ, *Macromolecules* **31**:5201–5205 (1998).
54 Lee DW, Seo EY, Cho SI and Yi CS, *J Polym Sci A: Polym Chem* **42**:2747–2755 (2004).